Integral cross sections and transport properties for electron-mercury scattering over a wide energy range (0.001-1000 eV) and reduced electric field range (0.01-1000 Td).

R. P. McEachran[1], G. J. Boyle[2],* and J. R. Machacek[1]
[1] *Research School of Physics, Australian National University, Canberra, A.C.T. 0200, Australia and*
[2] *College of Science and Engineering, James Cook University, Townsville, Queensland 4810, Australia*
(Dated: December 6, 2023)

We report calculations for electron-mercury scattering using a complex relativistic optical potential method. The energy range of this study is 0.001-1000 eV, with results for the elastic (and momentum-transfer) cross section, summed discrete electronic-state integral excitation cross sections and electron-impact ionization cross sections being presented. Here we obtain our cross sections from a single theoretical relativistic calculation. Since mercury is a heavy element, a relativistic treatment is very desirable. These *ab initio* calculations are compared to the cross section set recommended by Mirić *et al.* [1], which were developed from a variety of experimental and theoretical sources. Significant differences are noted between the total excitation and ionization cross sections, and the low-energy momentum-transfer cross section. Electron transport coefficients are subsequently calculated for reduced electric fields ranging from 0.01 to 1000 Td, using a multiterm solution of Boltzmann's equation. The results were compared against those calculated with the Mirić *et al.* set, and experimental measurements where possible. Overall, there is good agreement demonstrated between both cross section sets and experiment. The drift and diffusion coefficients calculated with the *ab initio* cross section set were generally lower than those calculated with the Mirić *et al.* set, at low reduced field strengths $E/N < 2$ Td, and vice versa for reduced fields strengths $E/N > 2$ Td. The ionisation coefficient calculated here was smaller than that of Mirić *et al.* and the experimental measurements over the full range of electric fields investigated.

I. INTRODUCTION

Mercury has been used to produce light since the discovery and subsequent development of the mercury vapour lamp [2]. The fluorescent lamp eventually became the backbone of the lighting industry due to the high efficiencies found using various gas combinations. The famous Franck-Hertz experiment [3] was originally demonstrated using electrons in mercury vapour. While light emitting diode (LED) technology has begun to displace vapour lamps, the role of discharge plasma chemistry in the fabrication of complex condensed-matter systems is still of utmost importance. In both cases, the detailed knowledge of the scattering cross section for a given atomic or molecular target is a critical starting point for any modeling procedure which hopes to produces predictive results. The level of detail of this work is the integral cross section including momentum transfer. This detail is required such that the transport of energy can accurately be predicted.

In a previous work, McEachran and Elford [4] calculated the the momentum-transfer cross section for low-energy electrons in mercury, < 3.0 eV, using a similar method to the one in this paper, and compared it to those derived from swarm measurements. Although excellent agreement was demonstrated for energies above 0.2 eV, there were significant differences at lower energies. The influence of mercury dimers was considered, as was the possible inadequacy of the theoretical description in this region, but ultimately the cause of the discrepancy is still unknown. In this work, the energy range is extended up to 1000 eV, and inelastic processes including excitations and ionization are included, along with elastic scattering. Recently, Mirić and co-workers [1] constructed a cross section set for electron transport in mercury, formed from a variety of theoretical and experimental data, and modified it to give very good agreement to the available drift and diffusion measurements over a wide range of reduced electric field strengths. They also considered the effect of mercury dimers on the transport, as well as their role in the phenomenon of negative differential conductivity. Whether a cross section set of similar high quality to the Mirić *et al.* recommended set (MRS) can be determined *ab initio* remains to be seen, and is one of the aims of this work.

We begin this paper by describing the theory for the cross section calculation using the complex relativistic optical potential (ROP) method, and the details of the transport theory and simulation in section II. The cross section calculations are presented and compared to the set of Mirić *et al.* in section III A. The corresponding transport properties are presented in section III B and compared with experimental measurements were available. Finally, the results are summarized in section IV.

II. THEORETICAL AND TRANSPORT SIMULATION DETAILS

A. Cross sections

In this work, the elastic, momentum-transfer and absorption cross sections were calculated using a complex

* Gregory.Boyle@my.jcu.edu.au

relativistic optical potential method in a similar manner to that outlined in the recent papers for zinc [5], indium [6] and cadmium [7]. The ROP method yields elastic, excitation and ionization cross sections that are in excellent agreement with experimental measurements of electron scattering in zinc, and good agreement for electron scattering in cadmium and indium, and thus similar results are expected here for mercury. A complete description of the ROP method is given in Chen *et al.* [8].

The ROP method is based upon an approximate solution of the Dirac scattering equations which contain both static and polarization potentials, the exchange terms, and a non-local optical potential to account for both excitation and ionization processes. The ground and excited-state wavefunctions of mercury were determined in a single configuration calculation using the multi-configuration Dirac-Fock (MCDF) program of Grant *et al.* [9]. The static potential was determined in the usual manner from the ground state Dirac-Fock orbitals of mercury while the non-local exchange interaction was included by antisymmetrizing the total scattering wavefunction. The polarization potential was determined by the polarized-orbital method [10, 11] and included the first 7 multipole potentials plus the monopole potential and the corresponding dynamic distortion polarization potential [12, 13]. Thus, asymptotically the polarization potential contained all terms up to and including those corresponding to r^{-16}.

The non-local optical potential is given by an expansion over the inelastic channels of the target atom. These inelastic channels include both excitation of the higher lying bound states and the single ionization of the valence $6s$ electron of mercury at 10.43 eV as well as ionization of the $5d$ and $5\bar{d}$ electrons of mercury at approximately 12.00 and 14.00 eV respectively. Eight excited bound states of mercury were included in the optical potential. These states included those where one of the electrons in the outer $6s$ valence shell was excited to higher lying states, namely, the $n\mathrm{p}^{1,3}P_1$ states with $n = 6$ to 9. The wavefunctions for these excited states were determined in a frozen-core approximation [14] and consequently, wavefunctions of the same overall symmetry, will be automatically orthogonal [15]. These states gave rise to 24 excitation channels. In the case of the excitation of individual lines, the total excitation cross section was calculated as follows. The total excitation cross section was determined without the line in question and this cross section was then subtracted from the total cross section including this line. In this manner, as much cross channel coupling between the various states was included. In the case of ionization, the 22 continuum states with an orbital angular momentum of the incident electron of 0 to 3 were included. This, in turn, gave rise to up to 106 ionization channels depending on the total angular momentum of the incident electron.

B. Transport simulations

The transport simulations are based on solutions to Boltzmann's equation employed here have been described extensively elsewhere [16–20]. We describe only the key points briefly here, and direct the reader to the references above for a more detailed account.

The transport of electrons in a gaseous system, such as a mercury vapour, subject to a uniform electric field **E**, can be described by the solution of the Boltzmann's equation for the phase-space distribution function f:

$$\frac{\partial f}{\partial t} + \boldsymbol{v}\cdot\nabla f + \frac{e\boldsymbol{E}}{m_e}\cdot\frac{\partial f}{\partial \boldsymbol{v}} = -J(f), \tag{1}$$

where $\boldsymbol{r}$, $\boldsymbol{v}$, and e denote the position, velocity, and charge of the electron, respectively. The collision operator $J(f)$ accounts for interactions between the electrons of mass m_e and the background medium.

If there are no strong gradients, then the space-time dependence of the phase-space distribution function can be projected onto the number density $n(\boldsymbol{r}, t)$ via the density gradient expansion [21],

$$\begin{aligned} f(\boldsymbol{r},\boldsymbol{v},t) = {} & nF(\boldsymbol{v}) - F^L(\boldsymbol{v})\frac{\partial n}{\partial z} \\ & - F^T(\boldsymbol{v})\left[\cos\phi\frac{\partial n}{\partial x} + \sin\phi\frac{\partial n}{\partial y}\right] \\ & + \sqrt{\frac{1}{3}}F^{2T}(\boldsymbol{v})\left[\frac{\partial^2 n}{\partial x^2} + \frac{\partial^2 n}{\partial y^2} + \frac{\partial^2 n}{\partial y^2}\right] \\ & + \sqrt{\frac{2}{3}}F^{2L}(\boldsymbol{v})\left[\frac{1}{2}\left(\frac{\partial^2 n}{\partial x^2} + \frac{\partial^2 n}{\partial y^2}\right) - \frac{\partial^2 n}{\partial y^2}\right] \\ & + \ldots, \end{aligned} \tag{2}$$

where ϕ is the azimuthal angle, and the superscripts L and T define quantities that are parallel and transverse to the electric field, respectively.

Solution of Boltzmann's equation (1) with the expansion (2) requires decomposition of the coefficients in velocity space through an expansion in (associated) Legendre polynomials, $P_l^m(\cos\theta)$ [22], i.e.,

$$F(\boldsymbol{v}) = \sum_{l=0}^{\infty} F_l(v)P_l^0(\cos\theta), \tag{3}$$

$$F^{L,2T,2L}(\boldsymbol{v}) = \sum_{l=0}^{\infty} F_l^{L,2T,2L}(v)P_l^0(\cos\theta), \tag{4}$$

$$F^T(\boldsymbol{v}) = \sum_{l=0}^{\infty} F_l^T(v)P_l^1(\cos\theta), \tag{5}$$

where θ denotes the angle relative to the electric field direction. Note that P_l^0 are just the standard Legendre polynomials. Boltzmann's equation can then be rewritten as a hierarchy of equations for these expansion coefficients [23].

The above represents a true multi-term solution of Boltzmann's equation, capable of accurately capturing

anisotropic scattering effects in velocity-space. This is important, as it is well known that the inclusion of inelastic processes can lead to a failure of low-order approximations [23–25]. In practice, the upper limit on the summations in equations (3)–(5) is set to some value, l_{max}, and then systematically increased until convergence of the relevant transport coefficients is achieved to the desired precision. In this work, $l_{max} = 5$ is required for the convergence of all transport coefficient considered to within 0.5%, over the full range of electric fields.

Solving for the (normalised) coefficients of equations (3)–(5) provides sufficient information to calculate transport properties [23], such as the flux drift velocity W, mean energy ϵ, flux longitudinal diffusion coefficient D^L and flux transverse diffusion coefficient D^T,

$$\epsilon = 2\pi m_e \int_0^\infty v^4 F_0(v) dv, \tag{6}$$

$$W = \frac{4\pi}{3} \int_0^\infty v^3 F_1(v) dv, \tag{7}$$

$$D^{L,T} = \frac{4\pi}{3} \int_0^\infty v^3 F_1^{L,T}(v) dv. \tag{8}$$

which are related to their bulk coefficients counterparts, the bulk drift velocity W_B, bulk longitudinal diffusion coefficient D_B^L, and bulk transverse diffusion coefficient D_B^T, via

$$W_B = W - 4\pi \int_0^\infty v^2 \nu_R(v) F_1(v) dv, \tag{9}$$

$$D_B^L = D^L - \frac{4\pi}{\sqrt{3}} \int_0^\infty v^2 \nu_R(v) \left[F_0^{2T}(v) - \sqrt{2} F_0^{2L}(v) \right] dv, \tag{10}$$

$$D_B^T = D^T - \frac{4\pi}{\sqrt{3}} \int_0^\infty v^2 \nu_R(v) \left[F_0^{2T}(v) + \frac{\sqrt{2}}{2} F_0^{2L}(v) \right] dv, \tag{11}$$

where $\nu_R(v)$ is the total reactive collision frequency. In the mercury vapour considered here, the only non-conservative process is electron-impact ionisation, and thus $\nu_R(v) = -\nu_{ion}(v) = -N v \sigma_{ion}(v)$. The electron mobility, μ, is given by

$$\mu = \frac{W_B}{E} \tag{12}$$

and is often reported in ratio with the bulk diffusion coefficient, as a proxy for the mean energy of the system.

Physically, the flux transport coefficients detail mean velocity and diffusion of the particles in the swarm, whereas the bulk transport coefficients are concerned with the spread about, and motion of, the swarm's centre of mass. When particle non-conservative processes are operative, such as ionisation, the bulk and flux coefficients can differ by several orders of magnitude, and even exhibit entirely different quantitative behaviour. It is important to recognize the difference, as it is the bulk and not the flux transport coefficients which are generally measured and tabulated in the vast majority of swarm experiment literature [25–27], thus we will focus on bulk properties here.

Finally, the net reaction rate R_{net} is related to the Townsend ionisation coefficient, α, by the expression

$$R_{net} \approx \alpha W_B - \alpha^2 D_B^L. \tag{13}$$

and we will report the Townsend ionisation coefficient rather than the net reaction rate in section III, for consistency with previous literature.

III. RESULTS AND DISCUSSION

A. cross sections

The electron-mercury scattering cross sections for the elastic momentum-transfer, total sum of excitations, and electron-impact ionisation processes, calculated using the ROP method described in section II A, are shown in Figure 1, along with the corresponding cross sections from Mirić *et al.* [1] (MRS). In the MRS, the excitations are reported as separate individual processes for excitation to the $^3P_0$, $^3P_1$, $^3P_2$, $^1P_1$, and $^1S_0$ states, as well as a lumped higher-excitation cross section. Although they are shown as totals in Figure 1 for comparison, we continue to treat each process separately when performing the transport calculations in the remainder of this work. In figure 1, the MRS ionisation coefficient has been extended to slightly lower energies than that shown in Mirić *et al.* [1], to make the behaviour near the threshold energy more clear. This has been achieved by supplementing the cross section with the near-threshold measurements from Bleakney [28] which have been interpolated and extrapolated.

The momentum-transfer cross sections agree very well for energies > 0.2 eV, but demonstrate a significant discrepancy at lower energies. The low-energy momentum-transfer cross section in the MRS comes from the swarm-derived results of England and Elford [29], and this discrepancy has been discussed previously [4]. The influence of mercury dimers as well as possible inadequacies in the theoretical description of the static and dynamic polarization at very low energies have both been considered as the source of the disagreement, but the issue remains unresolved.

The total excitation cross section and the electron-impact ionisation cross sections both demonstrate considerable differences. In particular, the ROP set exhibits a larger total excitation than the MRS, apart from close to the threshold energy of ≈ 5 eV. In contrast, the ionisation cross section from the ROP set is lower than the MRS ionisation, for almost all energies. The MRS ionisation cross section comes from the experiments of Smith [30], and is already lower than similar measurements from Jones [31], Bleakney [28], Liska [32], Harrison [33], as compiled by Kieffer and Dunn [34], further highlighting the discrepancy with the ROP result. It is

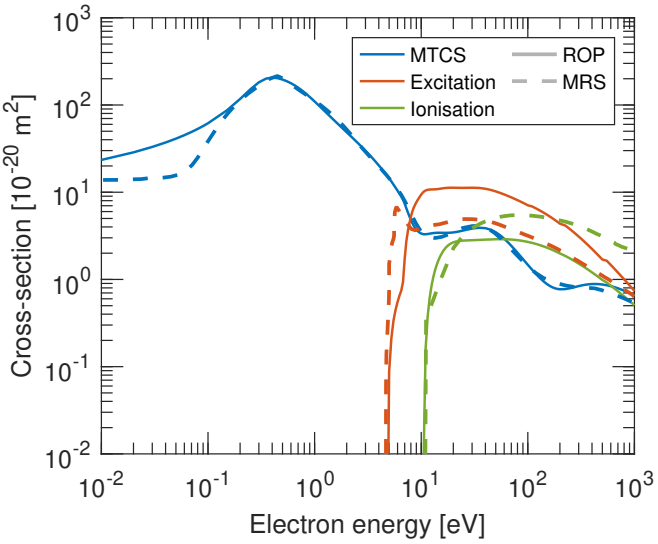

FIG. 1. cross sections for the elastic momentum-transfer (MTCS), sum of excitations (Excitation), and electron-impact ionisation (Ionisation) processes in mercury, calculated using the *ab initio* method described in Section II A (ROP, solid lines), and those digitized from Mirić *et al.* [1] (MRS, dashed lines).

interesting to note that the magnitude of the ROP ionisation is very similiar to the MRS excitation, while the ROP excitation is more similar in magnitude to the MRS ionisation, such that the total inelastic, i.e the sum of excitation and ionisation, is very comparable between the two sets. Thus, while the strength of the total inelastic interaction is very similar, the near-threshold dependencies are likely to impact the finer details of the transport. The affect of varying the relative strength of the excitation cross section effecting the transport of electrons has been demonstrated previously [25, 35].

The cross sections calculated using the ROP methodology described in section II A have been tabulated for a selection of energies in the range 0 to 1000 eV in Table I, for reference. Values for the total elastic are tabulated, along with the momentum-transfer, total excitation and ionisation, as displayed in the Figure 1.

B. Transport properties

Figure 2 displays transport properties (bulk drift velocity, mean energy, ratio of transverse diffusion coefficient to mobility, bulk longitudinal and transverse diffusion coefficients, and the ionisation coefficient) for an electron swarm in mercury vapour at 573 K. This temperature was chosen to be consistent with the experiments of England and Elford [29]. The calculated cross section set (Table I) and the set published by Mirić *et al.* [1] were used. The results consider the range of reduced electric fields E/N 10^{-2} Td to 10^{3} Td. Experimental measurements are also included here where available.

Generally, the ROP yields smaller values of the drift velocity and diffusion coefficients than those calculate with the MRS cross sections for low reduced electric fields $E/N < 2$, and vice versa at larger fields $E/N > 2$. At $E = 2$ Td, the mean energy of the electron swarm is approximately 1 eV. As shown in Figure 1, for energies below 1 eV, the electrons are in the purely elastic scattering regime, where the ROP momentum-transfer cross section is larger than the corresponding MRS profile. The enhanced momentum-transfer leads to reduced drift and diffusion, as demonstrated. At higher energies, above the excitation thresholds, the influence of the inelastic channels becomes important. As shown in Figure 1, the ROP exhibits a larger total excitation cross section, but a smaller ionisation cross section, with respect the MRS values. Noting that the MRS cross sections also feature individual excitations with specific threshold energies, the overall effect is to enhance the drift and diffusion at the higher electric fields, with respect to the MRS values.

In Figure 2 (a), the bulk drift velocity is shown. There is excellent agreement between the theoretical results using both sets of cross sections, and the the experimental results from England and Elford [29] and Klarfeld [36] over the reduced field range 0.1–10 Td. The experimental results from McCutchen [37] show significant differences at the low fields, and Mirić *et al.* [1] proposed that this may be due to the presence of trace amounts of mercury dimers. At very low fields < 0.1 Td, there is some divergence between the theoretical calculations using the two sets, but there is no experimental data here to compare. At high fields > 100 Td, the drift velocity calculated using the MRS agrees well with the experiments from Klarfeld, while the ROP set gives a slight overestimation. Overall, the ROP cross section set respectably reproduces the drift velocity of the MRS, and the experimental measurements.

The ratio of the the bulk transverse diffusion coefficient to electron mobility, D_B^T/μ, along with the mean energy, ϵ, are shown in In Figure 2 (b). Despite significant differences between the ROP and MRS being demonstrated, the agreement with the available experimental data for the two sets is comparable, with the larger results of ROP set agreeing better with the experiments of Klarfeld [36], while the lower MRS values agrees better with the experiments of Hayes and Wojaczek [38]. Both simulated sets are in good agreement with the measurements of Ovcharenko and Chernyshev [39]. The mean energy is also shown for reference, and demonstrates similar behaviour to the characteristic energy, $\frac{3}{2}D_B^T/\mu$, justifying the latter's use as a proxy for the mean energy of the electron distribution.

In Figure 2 (c), the bulk longitudinal and transverse diffusion coefficients are shown. There is no available experimental data to evaluate accuracy. There is excellent agreement in the longitudinal coefficients in the field range $E - N = 0.1 - 2$ Td. Otherwise, the ROP gives larger values of the longitudinal and transverse diffusion coefficients than the MRS for low fields, and vice versa

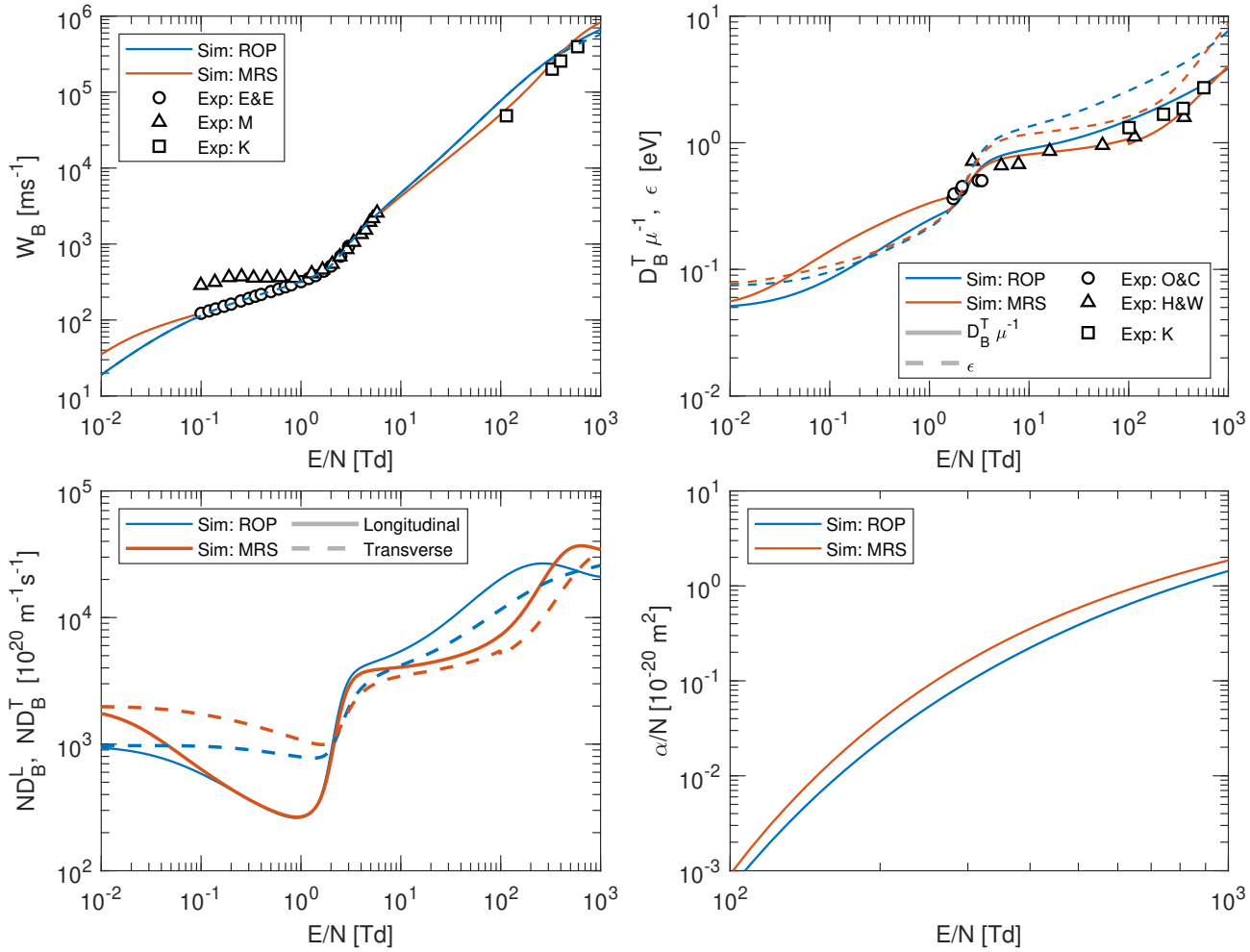

FIG. 2. Comparison between transport simulated using the *ab initio* cross section set described in Section II A and tabulated in in Table I (Sim: ROP, blue), and that using the cross section set of Mirić *et al.* [1] (Sim: MRS, red). The transport properties are defined in equations (6)–(12). **a)** Bulk drift velocity. The experimental data is from England and Elford 1991 [29] (Exp: E&E, circles), McCutchen 1958 [37] (Exp: M, triangles) and Klarfeld 1958 [36] (Exp: K, squares), respectively. **b)** Ratio of bulk transverse diffusion to mobility (sold lines), and mean energy (dashed lines). The experimental data for the characteristic energy is from Ovcharenko and Chernyshev 1970 [39] (Exp: O&C, circles), Hayes and Wojaczek 1963 [38] (Exp: H&W, triangles) and Klarfeld 1938 [36] (Exp: K, squares), respectively. **c)** The longitudinal (solid lines) and transverse (dashed lines) diffusion coefficients. **d)** Ionisation coefficient. The experimental data is from Overton and Davies 1968 [40] (Exp: O&D, circles), along with the recommended values of Raju 2011 [41], determined from various sources (Rec: R, triangles).

at higher fields, which is a reflection of the differences in the cross section sets, as discussed above.

The Townsend ionisation coefficient is displayed in Figure 2 (d). The ROP values are consistently smaller than the experimental measurements of Overton and Davies [40], the recommended values of Raju [41], and the MRS values, the latter of which is a direct consequence of the smaller ionisation cross section, shown in Figure 1. Note that the MRS cross sections, specifically the excitations, were modified [1] from earlier cross sections to better reproduce the recommended ionisation coefficients of Raju.

Overall, the ROP cross section set presented here reproduces the (limited) experimental data for the drift velocity and diffusion coefficients well, while consistently underestimating the ionisation coefficient. We again emphasize that this approach has no free parameters, i.e. that it represents an *ab initio* method. The transport properties are comparable with, though showing distinct differences to, the cross section set recommended by Mirić *et al.* [1], which was compiled from theoretical and experimental sources and modified to give very good agreement to the available experimental data.

TABLE I. A representative selection of the calculated cross sections for total elastic (Elastic), momentum-transfer (MTCS), sum of all discrete excitations (Excitation), and electron-impact ionization (Ionisation), for electron scattering from mercury. Calculations have been performed using the method described in Section II A, and coincide with the profiles shown in Figure 1.

Energy [eV]	Elastic [10^{-20} m^2]	MTCS [10^{-20} m^2]	Excitation [10^{-20} m^2]	Ionisation [10^{-20} m^2]	Energy [eV]	Elastic [10^{-20} m^2]	MTCS [10^{-20} m^2]	Excitation [10^{-20} m^2]	Ionisation [10^{-20} m^2]
0	12.4	12.4	0	0	15	6.62	3.43	11.0	1.82
1×10^{-3}	15.1	15.8	0	0	16	6.34	3.42	11.1	2.10
2×10^{-3}	16.1	17.2	0	0	17	6.17	3.42	11.2	2.32
5×10^{-3}	18.2	20.1	0	0	18	6.08	3.43	11.2	2.48
1×10^{-2}	20.4	23.5	0	0	19	6.06	3.44	11.3	2.59
2×10^{-2}	23.6	28.7	0	0	20	6.09	3.46	11.3	2.66
5×10^{-2}	30.6	41.1	0	0	21	6.16	3.49	11.2	2.71
1×10^{-1}	42.6	61.7	0	0	22	6.26	3.53	11.2	2.74
2×10^{-1}	84.7	117	0	0	23	6.38	3.57	11.2	2.77
3×10^{-1}	153	182	0	0	24	6.52	3.61	11.2	2.78
4×10^{-1}	199	206	0	0	25	6.67	3.65	11.2	2.79
5×10^{-1}	209	196	0	0	30	7.49	3.83	11.3	2.82
6×10^{-1}	206	178	0	0	35	8.24	3.91	11.2	2.84
7×10^{-1}	198	158	0	0	40	8.79	3.87	11.0	2.86
8×10^{-1}	186	140	0	0	45	9.16	3.71	10.6	2.87
9×10^{-1}	175	124	0	0	50	9.36	3.48	10.2	2.89
1	163	110	0	0	55	9.44	3.21	9.82	2.90
1.1	152	98.2	0	0	60	9.43	2.93	9.43	2.89
1.2	143	88.6	0	0	65	9.38	2.67	9.07	2.88
1.3	134	80.6	0	0	70	9.30	2.43	8.72	2.87
1.4	126	73.8	0	0	75	9.20	2.21	8.41	2.85
1.5	119	68.1	0	0	80	9.09	2.02	8.11	2.82
1.6	113	63.1	0	0	85	8.98	1.86	7.83	2.79
1.7	108	58.8	0	0	90	8.87	1.71	7.57	2.76
1.8	102	55.0	0	0	95	8.75	1.58	7.32	2.73
1.9	97.7	51.7	0	0	100	8.64	1.47	7.09	2.69
2	93.5	48.7	0	0	110	8.42	1.29	6.86	2.62
2.5	76.4	37.4	0	0	120	8.21	1.15	6.50	2.55
3	64.0	29.9	0	0	130	8.00	1.04	6.16	2.47
3.5	54.6	24.5	0	0	140	7.79	9.54×10^{-1}	5.85	2.40
4	47.1	20.3	0	0	150	7.58	8.91×10^{-1}	5.56	2.32
4.5	41.1	17.0	0	0	160	7.38	8.45×10^{-1}	5.29	2.25
5	35.6	14.5	8.76×10^{-2}	0	170	7.18	8.13×10^{-1}	5.03	2.18
5.5	31.2	12.2	3.40×10^{-1}	0	180	6.98	7.91×10^{-1}	4.79	2.11
6	27.6	10.4	5.52×10^{-1}	0	190	6.78	7.78×10^{-1}	4.57	2.05
6.5	24.5	8.93	7.44×10^{-1}	0	200	6.59	7.71×10^{-1}	4.36	1.99
7	21.6	7.40	1.73	0	250	5.73	7.94×10^{-1}	3.75	1.73
7.5	19.3	5.86	3.59	0	300	5.06	8.39×10^{-1}	3.11	1.52
8	17.3	4.82	5.22	0	350	4.55	8.71×10^{-1}	2.62	1.35
8.5	15.6	4.14	6.63	0	400	4.16	8.85×10^{-1}	2.23	1.20
9	14.1	3.73	7.66	0	450	3.87	8.85×10^{-1}	1.93	1.09
9.5	12.8	3.50	8.55	0	500	3.63	8.75×10^{-1}	1.69	9.87×10^{-1}
10	11.7	3.36	9.39	0	550	3.45	8.59×10^{-1}	1.64	9.22×10^{-1}
10.5	10.8	3.30	10.1	7.30×10^{-3}	600	3.29	8.38×10^{-1}	1.47	8.50×10^{-1}
11	9.94	3.29	10.5	1.61×10^{-1}	650	3.16	8.16×10^{-1}	1.32	7.87×10^{-1}
11.5	9.24	3.32	10.7	3.80×10^{-1}	700	3.04	7.92×10^{-1}	1.20	7.31×10^{-1}
12	8.64	3.35	10.7	6.13×10^{-1}	750	2.94	7.67×10^{-1}	1.09	6.83×10^{-1}
12.5	8.13	3.38	10.8	8.48×10^{-1}	800	2.86	7.42×10^{-1}	1.00	6.39×10^{-1}
13	7.70	3.40	10.8	1.07	850	2.78	7.18×10^{-1}	9.24×10^{-1}	6.01×10^{-1}
13.5	7.35	3.42	10.8	1.28	900	2.71	6.94×10^{-1}	8.54×10^{-1}	5.66×10^{-1}
14	7.05	3.42	10.8	1.48	950	2.64	6.70×10^{-1}	7.93×10^{-1}	5.34×10^{-1}
14.5	6.82	3.43	10.9	1.66	1000	2.58	6.47×10^{-1}	7.38×10^{-1}	5.06×10^{-1}

IV. SUMMARY

We have determined from *ab initio* ROP calculations a set of cross section data for electron scattering from mercury, including the elastic, elastic momentum-transfer, the sum of discrete excited electronic-states and the electron-impact ionization, processes. This cross section set was compared to the set recommended by Mirić *et al.* [1], which was assembled from a combination of theoretical and experimental sources to give very good agreement to the available swarm measurement data. The two cross section sets demonstrated significant differences in the magnitude of the total excitation and ionisation cross sections, as well as with the momentum-transfer cross section at very low energies. The latter discrepancy has been long known [4], but not yet resolved. When comparing the corresponding transport coefficients (W_B, ϵ, D_B^T/μ, ND_B^L, ND_B^T and α/N) for electrons in mercury vapour at 573 K, subject to a uniform external electric field, calculated from a multi-term Boltzmann equation solution, the two sets agreed well with each other, and with the limited available experimental measurements, for the drift velocity and diffusion coefficients over the full range of reduced electric field strengths $0.01 - 1000$ Td. Generally the transport coefficients calculated using the *ab initio* cross section set were lower than those calculated using the Mirić *et al.* set for fields $E/N < 2$ Td, and vice versa for fields $E/N > 2$ Td. The ROP ionisation coefficient, however, consistently underestimated the direct experimental and experimentally-derived values. This may warrant further future experiments for measuring the electron-impact ionisation cross section of mercury.

Acknowledgments

The authors wish to thank M. Brunger for the many years of rich and fruitful collaboration. The authors also wish to acknowledge the supprt of the Australian Research Council.

Author contributions

All authors contributed to the conceptualization, calculations, analysis and the writing of this manuscript.

Data availability statement

A representative selection of data is presented in Table 1. Data will be made available upon reasonable request.

[1] J. Mirić, I. Simonović, Z. L. Petrović, R. D. White, and S. Dujko, Electron transport in mercury vapor: cross sections, pressure and temperature dependence of transport coefficients and ndc effects, The European Physical Journal D **71**, 1 (2017).

[2] M. B. Rubin, The development of the mercury lamp, Bulletin for the History of Chemistry **35**, 105 (2010).

[3] J. Franck and G. Hertz, Ueber zusammenstoesse zwischen elektronen und den molekuelen des quecksilberdampfes und die ionisierungsspannung desselben, Physikalische BlÃ¤tter **23**, 294 (1967).

[4] R. P. McEachran and M. T. Elford, The momentum transfer cross section and transport coefficients for low energy electrons in mercury, Journal of Physics B: Atomic, Molecular and Optical Physics **36**, 427 (2003).

[5] R. P. McEachran, B. P. Marinković, G. García, R. D. White, P. W. Stokes, D. B. Jones, and M. J. Brunger, Integral Cross Sections for Electron–Zinc Scattering over a Broad Energy Range (0.01–5000 eV), Journal of Physical and Chemical Reference Data **49**, 013102 (2020).

[6] K. R. Hamilton, O. Zatsarinny, K. Bartschat, M. S. Rabasović, D. Šević', B. P. Marinković, S. Dujko, J. Atić, D. V. Fursa, I. Bray, R. P. McEachran, F. Blanco, G. García, P. W. Stokes, R. D. White, D. B. Jones, L. Campbell, and M. J. Brunger, Recommended Cross Sections for Electron–Indium Scattering, Journal of Physical and Chemical Reference Data **50**, 013101 (2021).

[7] B. P. Marinković, R. P. McEachran, D. V. Fursa, I. Bray, H. Umer, F. Blanco, G. García, M. J. Brunger, L. Campbell, and D. B. Jones, Cross Sections for Electron Scattering from Cadmium: Theory and Experiment, Journal of Physical and Chemical Reference Data **52**, 023102 (2023).

[8] S. Chen, R. P. McEachran, and A. D. Stauffer, Ab initio optical potentials for elastic electron and positron scattering from the heavy noble gases, Journal of Physics B: Atomic, Molecular and Optical Physics **41**, 025201 (2008).

[9] I. Grant, B. McKenzie, P. Norrington, D. Mayers, and N. Pyper, An atomic multiconfigurational dirac-fock package, Computer Physics Communications **21**, 207 (1980).

[10] R. P. McEachran, A. G. Ryman, A. D. Stauffer, and D. L. Morgan, Positron scattering from noble gases, Journal of Physics B: Atomic and Molecular Physics **10**, 663 (1977).

[11] R. P. McEachran, D. L. Morgan, A. G. Ryman, and A. D. Stauffer, Positron scattering from noble gases: corrected results for helium, Journal of Physics B: Atomic and Molecular Physics **11**, 951 (1978).

[12] D. J. R. Mimnagh, R. P. McEachran, and A. D. Stauffer, Elastic electron scattering from the noble gases including dynamic distortion, Journal of Physics B: Atomic, Molecular and Optical Physics **26**, 1727 (1993).

[13] R. P. McEachran and A. D. Stauffer, Dynamic distortion effects in electron-atom scattering, Journal of Physics B: Atomic, Molecular and Optical Physics **23**, 4605 (1990).

[14] R. P. McEachran and M. Cohen, The frozen-core approximation with a nonempirical polarisation potential: the sodium isoelectronic sequence, Journal of Physics B:

Atomic and Molecular Physics **16**, 3125 (1983).
[15] R. P. McEachran, C. E. Tull, and M. Cohen, Frozen core approximation for atoms and atomic ions, Canadian Journal of Physics **46**, 2675 (1968).
[16] R. E. Robson, R. D. White, and M. Hildebrandt, *Fundamentals of Charged Particle Transport in Gases and Condensed Matter* (CRC Press, 2017).
[17] G. Boyle, *The modelling of non-equilibrium light lepton transport in gases and liquids*, Ph.D. thesis, James Cook University (2015).
[18] G. J. Boyle, W. J. Tattersall, D. G. Cocks, R. P. McEachran, and R. D. White, A multi-term solution of the space–time Boltzmann equation for electrons in gases and liquids, Plasma Sources Science and Technology **26**, 024007 (2017).
[19] G. J. Boyle, M. J. E. Casey, D. G. Cocks, R. D. White, and R. J. Carman, Thermalisation time of electron swarms in xenon for uniform electric fields, Plasma Sources Science and Technology **28**, 035009 (2019).
[20] G. J. Boyle, P. W. Stokes, R. E. Robson, and R. D. White, Boltzmann's equation at 150: Traditional and modern solution techniques for charged particles in neutral gases, The Journal of Chemical Physics **159**, 024306 (2023).
[21] K. Kumar, H. Skullerud, and R. E. Robson, Kinetic theory of charged particle swarms in neutral gases, Australian Journal of Physics **33**, 343 (1980).
[22] M. Abramowitz and I. Stegun, *Handbook of mathematical functions* (Dover Publications Inc., 1972).
[23] R. Robson and K. Ness, Velocity distribution function and transport coefficients of electron swarms in gases: spherical-harmonics decomposition of Boltzmann's equation, Physical Review A **33**, 2068 (1986).
[24] R. D. White, R. E. Robson, B. Schmidt, and M. A. Morrison, Is the classical two-term approximation of electron kinetic theory satisfactory for swarms and plasmas?, Journal of Physics D: applied physics **36**, 3125 (2003).
[25] Z. L. Petrović, S. Dujko, D. Marić, G. Malović, Z. Nikitović, O. Sasić, J. Jovanović, V. Stojanović, and M. Radmilović-Radjenović, Measurement and interpretation of swarm parameters and their application in plasma modelling, Journal of Physics D: Applied Physics **42**, 194002 (2009).
[26] R. Robson, Transport phenomena in the presence of reactions: definition and measurement of transport coefficients, Australian journal of physics **44**, 685 (1991).
[27] M. J. E. Casey, P. W. Stokes, D. G. Cocks, D. Bosnjakovic, I. Simonovic, M. J. Brunger, S. Dujko, Z. L. Petrovic, R. E. Robson, and R. D. White, Foundations and interpretations of the pulsed-townsend experiment, Plasma Sources Science and Technology **30**, 035017 (2021).
[28] W. Bleakney, Probability and critical potentials for the formation of multiply charged ions in hg vapor by electron impact, Phys. Rev. **35**, 139 (1930).
[29] J. England and M. Elford, Momentum transfer cross section for electrons in mercury vapour derived from drift velocity measurements in mercury vapour? gas mixtures, Australian journal of physics **44**, 647 (1991).
[30] P. T. Smith, The ionization of mercury vapor by electron impact, Phys. Rev. **37**, 808 (1931).
[31] T. J. Jones, Probability of ionization of mercury vapor by electron impact, Phys. Rev. **29**, 822 (1927).
[32] J. W. Liska, Efficiencies of ionization of helium and mercury by electron impact at high voltages, Phys. Rev. **46**, 169 (1934).
[33] H. Harrison, *The Experimental Determination of Ionization Cross-of Gases Under Electron Impact.*, Ph.D. thesis, The Catholic University of America (1957).
[34] L. J. Kieffer and G. H. Dunn, Electron impact ionization cross-section data for atoms, atomic ions, and diatomic molecules: I. experimental data, Rev. Mod. Phys. **38**, 1 (1966).
[35] Z. L. Petrović, M. Suvakov, Z. Nikitović, S. Dujko, O. Sasić, J. Jovanović, G. Malović, and V. Stojanović, Kinetic phenomena in charged particle transport in gases, swarm parameters and cross section data*, Plasma Sources Science and Technology **16**, S1 (2007).
[36] B. Klarfeld, The positive column of a gaseous discharge, Tech. Phys. USSR **5**, 913 (1938).
[37] C. W. McCutchen, Drift velocity of electrons in mercury vapor and mercury vapor—co_2 mixtures, Phys. Rev. **112**, 1848 (1958).
[38] E. Hayes and K. Wojaczek, Determination of the averaged diffuse electron–mercury atom cross section, Beitr. Plasmaphys. **3**, 74 (1963).
[39] V. Ovcharenko and S. M. Chernyshev, Determination of the averaged diffuse electron–mercury atom cross section, Teplofizika vysokikh temperatur **8**, 716 (1970).
[40] G. D. N. Overton and D. E. Davies, Journal of Physics D: Applied Physics **1**, 882 (1968).
[41] G. G. Raju, *Gaseous electronics: tables, atoms, and molecules* (CRC Press, 2011).